Article

The Effect of Intermediate Principal Stress on Compressive Strength of Different Cement Content of Cement-Stabilized Macadam and Different Gradation of AC-13 Mixture

Hong-xin Guan [1,2,*], Hao-qing Wang [3], Hao Liu [1,3], Jia-jun Yan [1,4] and Miao Lin [1,5]

[1] School of Traffic & Transportation Engineering, Changsha University of Science & Technology, Changsha 410114, Hunan, China; crbcliuh1@gmail.com (H.L.); yanjiajun229@hotmail.com (J.-j.Y.); m170510015@fzu.edu.cn (M.L.)

[2] State Engineering Laboratory of Highway Maintenance Technology, Changsha University of Science & Technology, Changsha 410114, Hunan, China

[3] China Road & Bridge Corporation, Beijing 100011, China; whqcrb@hotmail.com

[4] Hubei Expressway Business Development Co. Ltd., Wuhan 430050, Hubei, China

[5] School of Civil Engineering, Fuzhou University, Fuzhou 350116, Fujian, China

[*] Correspondence: ghx_cs@csust.edu.cn; Tel.: +86-0731-8525-8249

check for updates

Abstract: Since the effect of intermediate principal stress on the strength of pavement materials is not entirely clear so far, a proprietary true triaxial apparatus was developed to simulate the spatial status of principal stresses to conduct compressive strength tests on different gradations of AC-13, different cement contents of cement-stabilized macadam. With the same minimum principal stress, the triaxial compressive strengths of cube specimens under different intermediate principal stresses were compared. The results indicate that, as the intermediate principal stress increases, the compressive strength of the specimen increases and then decreases; different gradations of AC-13 do not show much difference in triaxial compressive strength while different cement contents of cement-stabilized macadam indicate considerable difference. Analysis results suggest significant effect of intermediate principal stress on the compressive strength of pavement materials: for AC-13, the coarser the gradation, the greater the effect of intermediate principal strength on its strength; for cement-stabilized Macadam, the higher the cement content, the greater the effect of intermediate principal stress. Strength model analysis results suggest that Double-Shear-Corner Model is more suitable to characterize cement-stabilized macadam's strength performance compared to the Mohr–Coulomb model and Double-Shear Model.

Keywords: intermediate principle stress; compressive strength; true-triaxial; asphalt mixtures; cement stabilized macadam; gradation; cement content

1. Introduction

Strength is one of the main indicators for evaluating the mechanical properties of pavement materials. The normal laboratory test methods to evaluate the strength of pavement materials include uniaxial compression test, uniaxial tensile test, Brazilian splitting test, bending test and the conventional triaxial test. However, any point inside a pavement is in a three-dimensional stress state. The conventional triaxial test is very popular because of its complex stress state. However, the intermediate principal stress is always equal to the minimum stress for the conventional triaxial test. It means that the intermediate principal stress effect can't be considered. Therefore, it is necessary to study how the pavement materials' strength can be influenced by intermediate principal stress.

Many researchers have carried out true triaxial tests for materials such as rock, soil, and concrete, which obtained highly significant achievements. For example, Shao-kun carried out the constant water content triaxial tests on Yunnan red clay to study soil-water characteristics and shear strength [1]. The true triaxial test performed by Hang-zhou for joint rock mass shows that the established strength criteria can precisely reflect the strength of the rock mass [2]. Wang carried out biaxial and triaxial tests for mass concrete and put forward the failure criteria of mass concrete in principal stress space and octahedral stress space [3]. Saurav carried out a true triaxial test on cubical sample of plain cement concrete. The results show that the ratio of intermediate and minor principal stress had an incremental effect on the strength of the concrete [4]. Huai-shuai studied the triaxial compressive strength and deformation of air-entrained concrete under freeze-thaw cycles [5]. Rukhaiyar carried out polyaxial tests on cubical specimens of sandstone. The results show that the intermediate principle stress effect can not be ignored, and modified Mohr–Coulomb criterion is suitable for sandstone [6]. Jian-hua conducted a true triaxial test on different materials in the context of new mixed-boundary conditions to identify their stress-strain and strength under triaxial stress [7]. Wei-cheng conducted a true triaxial test on gravel and coarse-grained soil materials and discovered that the rules reflected by the Lade-Duncan criterion is the closest to test results [8,9]. Undrained triaxial and simple shear tests were carried out by Eghbali under the condition of different cement dosages and different stress paths [10]. Triaxial compression tests were carried out by Jia-jia on the high-performance concrete specimens with different mixing proportions [11]. Under conditions of different stress ratios, the triaxial tests on recycled aggregate concrete were carried out by Zhen-jun [12]. By comparing the true triaxial test and the discrete element analysis method, Daraporn studied the effect of different intermediate principal stress ratio on the mechanical properties of granular materials [13]. Triaxial compression tests were carried out by Yang to study the influence of intermediate principal stress ratio b on the stress-dilatancy relational of coarse granular soil [14]. However, little has been reported regarding true triaxial test on asphalt mixture or cement-stabilized materials. Hong-xin conducted a triaxial compressive strength test on modified asphalt AC-13 mixture with an apparatus allowing triaxial independent loading [15]. Li-jun qualitatively validated the applicability of twin-shear strength for asphalt mixture using a proprietary plane strain apparatus [16]. Lin-bing verified the anisotropy of asphalt mixture through modulus variation during true-triaxial independent loading test [17]. Xin-jiang compared the respective stress–strain curves of maximum, intermediate and minor principal stresses for the true triaxial test on cemented soil [18]. Tuo carried out triaxial tests on hollow cylinder asphalt mixture specimen at tensile-compress and compress–compress state. An octahedral failure criterion was developed for asphalt mixture [19,20]. Qun compared the strength analysis theory with the traditional theory [21].

Compared with the research in the geotechnical field [1–14], despite some research on some pavement materials strength under complex stresses being reported [15–21], it is necessary to study the true triaxial strength of the two most important pavement materials in China more deeply: asphalt mixture and cement-stabilized macadam with respect to, for example, the impact of intermediate principal stress on different gradations of the same type of mixtures. These studies will help to more accurately guide the pavement materials' composition design and even to provide a solution for early cracking of pavements.

In this paper, a true triaxial test will be conducted on different gradations of asphalt mixture and cement-stabilized macadam, using a simple proprietary true triaxial apparatus, to examine the effect of intermediate principal stress on their strengths.

2. Test Method

2.1. Test Apparatus

A simple true triaxial apparatus designed by the project team, consisting of a reactive frame and a hydraulic system, as shown in Figures 1 and 2, was used for the test. The reaction frame serves as

the support while the hydraulic system supplies the power needed. Different from other common triaxial apparatuses, this apparatus can provide triaxial independent loading forces, which allows any compressive stress combination of the three principal stresses.

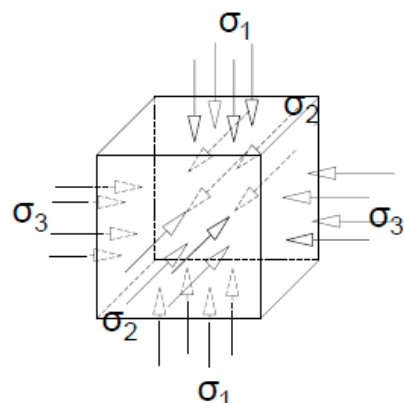**Figure 1.** Self-developed true triaxial test machine.

Figure 2. Schematic diagram for loading on specimen.

2.2. Test Conditions

2.2.1. Test Temperature

For ease of analysis, the compressive stress is assumed as positive while the tensile stress is negative. All sides of the specimen in this paper are pressed, so the stresses on it are all recorded as positive. Under principal stress space state, there are only three mutually perpendicular normal stresses which are also called principal stresses. When the three-way principal stress is sorted from large to small, they are called maximum principal stress, intermediate principal stress and minimum principal stress, respectively, which are represented by σ_1, σ_2 and σ_3, respectively.

Asphalt mixture is closer to brittle solids at low temperature. Compared with the relatively high temperature condition, asphalt mixture's creep effect at low temperature has less influence on its strength. According to the test temperature of Low Temperature Bending Test for asphalt mixture being set at $-10\ ^\circ$C in Chinese Specifications, test temperature in this paper was set at $-10\ ^\circ$C.

As for cement-stabilized macadam, it is less sensitive to temperature and the recommended test temperature for cement-stabilized materials in relevant test specifications is 20 $^\circ$C, regardless of it being a curing test or an unconfined compressive strength or indirect tensile test. The test temperature was set at 20 $^\circ$C in this paper triaxial compressive strength tests on cement-stabilized macadam.

2.2.2. Loading Rate

It is generally known that the strength of the asphalt mixture will increase with the increase of loading rate when all the other conditions are the same. In view of the test specifications for asphalt mixtures in China, abroad and particularly in these tests, the subsequent triaxial strength tests on AC-13 asphalt mixture were conducted at the loading rate of 18 mm/min.

Since Chinese test specifications recommend a loading rate of 1 mm/min for unconfined compressive strength and splitting strength of cement-stabilized macadam, the loading rate of a true-triaxial compressive test on cement-stabilized material was set at 1 mm/min.

2.2.3. Loading Path

The proprietary test apparatus features a simple loading path. First, the σ_3 and σ_2 control values are set. Then, the three principal stresses are loaded synchronously at the same loading rate. When σ_3 reaches its predetermined value, it is held while continuing to increase σ_2 and σ_1. When σ_2 reaches its predetermined value, σ_3 and σ_2 are held while continuing to increase σ_1 until the specimen eventually fails. The failure stress then is σ_1.

2.3. Specimen Preparation

Cubic specimens were used in the tests. The asphalt mixture specimen was first rotationally compacted into a Φ150 mm, 100 mm-tall cylinder before it was cut by an infrared-ray cutter into an 88 mm × 88 mm × 88 mm specimen.

Since there is an optimal content of bituminous in asphalt mixture, only the effects of aggregate gradation will be discussed here. Gradations of asphalt mixture AC-13 used for this test are listed in Table 1. The bituminous type was 70#A class made in China. In Table 1, AC-13F*, AC-13M and AC-13C means separately fine gradation, median gradation and course gradation within the range of AC-13 gradation [22]. The bitumen aggregate ratio of AC-13F*, AC-13M and AC-13C is 5.05%, 4.85% and 4.8%, respectively.

Table 1. The aggregate passing rate (%) from sieve pore for Asphalt Mixture.

Sieve Pore (mm) / Mixture Type	16	13.2	9.5	4.75	2.36	1.18	0.6	0.3	0.15	0.075
AC-13F*	100.0	97.3	75.8	61	38.5	23.6	17.3	9.6	5.8	3.7
AC-13M	100	95	76.5	53	37	26.5	19	13.5	10	6
AC-13C	100	97.7	80	53.3	30.4	19.3	14.4	8.5	5.4	4

The cement-stabilized macadam specimens were molded into 15 mm × 15 mm × 15 mm specimen with static pressure. After it was prepared, the cube was delivered into a standard curing room and cured for 90 d under the temperature of 20 °C and humidity of 95% as specified by Chinese standard [23].

Since there is not an optimal content of cement for cement-stabilized macadam, and cement usage is often paid more attention, only the effects of cement content will be discussed here. The gradation of cement-stabilized macadam used for this test is listed in Table 2. The cement content for this paper includes 3.5%, 4.5% and 5.5% with the same aggregate gradation.

Table 2. The aggregate gradation of cement-stabilized macadam.

Sieve pore (mm)	31.5	19	9.5	4.75	2.36	0.6	0.075
Aggregate passing rate (%)	100	94.9	74.19	28.2	19.2	11.2	1.3

3. Effect of Intermediate Principal Stress on the Compressive Strength of Asphalt Mixture

In order to prove the suitability of the test apparatus as shown in Figure 1, compressive strength tests on AC-13C were carried out with the self-developed true triaxial test machine at the condition of $\sigma_2 = \sigma_3$, as this stress state is similar to that of conventional triaxial test. The test result is shown in Figure 3. In Figure 3, the Mohr stress circle curve 1–9 was obtained under the condition of $\sigma_2 = \sigma_3 = 0$, 1, 2, 3, 4, 5, 6, 7, 8, 9 MPa, respectively. The vertical axis is the maximum shear stress and the horizontal axis is the normal stress at the plane of the maximum shear stress.
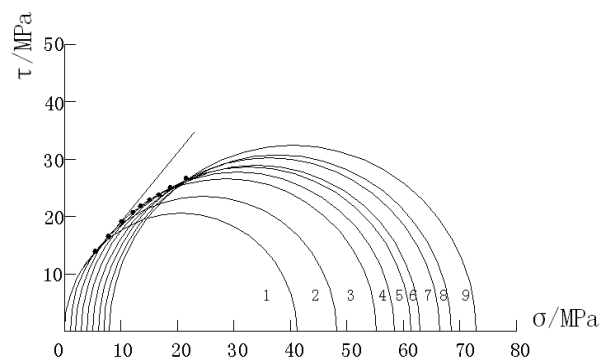

Figure 3. The Mohr stress circles and shear strength envelope of AC-13C.

Figure 3 shows that the shear strength envelope of AC-13C gradually bends as the stress $\sigma3$ increases. This changing rule is consistent with the study results of reference [24].

Under the condition that the minimum principal stress $\sigma_3 = 2$MPa and σ_2 varied between the minimum and the maximum principal stresses, triaxial compressive strength tests were carried out on AC-13 mixture specimens as shown in Table 1. The results are shown in Figures 4 and 5.
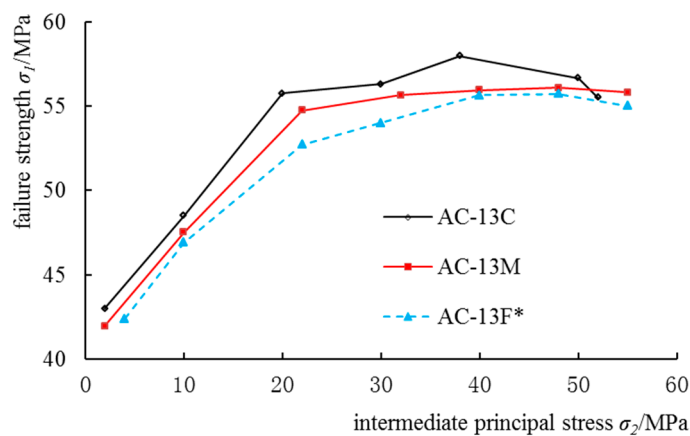

Figure 4. AC-13 triaxial compressive strength changing with intermediate principal stress.

Figure 4 shows that, in case there are compressive stresses in three directions and σ_3 is a constant, the strength of the asphalt mixture changes parabolically as the intermediate principal stress increases. This indicates that the intermediate principal stress has an effect on the failure strength of the asphalt mixture, and there is an interval effect involved. In addition, when the asphalt mixture specimen is under the true triaxial conditions, the stresses at all the failure points are higher than the ordinary uniaxial compressive strength, indicating that the existence of the intermediate principal stress can increase the compressive strength of the asphalt mixture dramatically.

To reflect the effect of intermediate principal stress on the failure strength of the materials, an intermediate principal stress influence factor b was defined as $b = \frac{\sigma_2 - \sigma_3}{\sigma_1 - \sigma_3}$. When $\sigma_2 = \sigma_3$, $b = 0$; when $\sigma_1 = \sigma_2$, $b = 1$. Under the test condition of σ_3 be a constant, if the setting value of σ_2 gradually increases

from the value of σ_3, the factor *b* can intuitively reflect the level of intermediate principal stress in the three principal stresses.

Based on the test results, a figure was developed to show the impact of the intermediate principal stress factor on the failure strength of AC13 mixture, as shown in Figure 5.
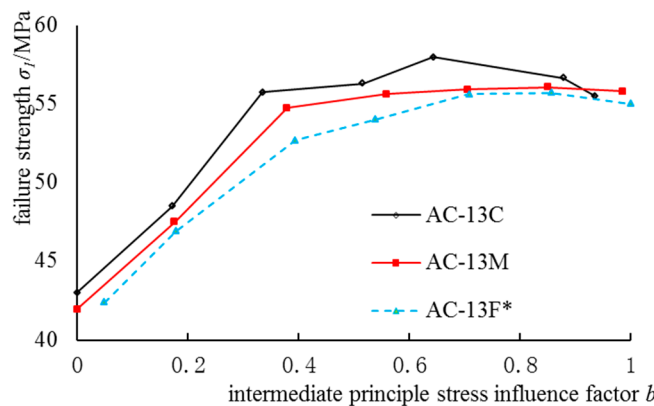

Figure 5. Intermediate principle stress influence factor b vs. strength of different gradation AC-13 mixture.

Figure 5 shows that the effect of intermediate principal stress factor b on the failure strength of AC-13 mixture also exists, and the failure strength tends to be rising followed by a fall. The three curves are quite similar to each other, which suggest that, for the same type of asphalt mixture, gradation differences do not make much difference to its triaxial strength.

To further reflect how intermediate principal stress affects the strength of different gradations of AC mixture, the intermediate principal stress influence factor at the peak point, b_m, and the failure stress will be used. If b_m is small while the failure stress is large, the curve of σ_2 arriving at the peak point from σ_3 is steep. That is, the steeper the curve, the greater the effect of intermediate principal stress on the failure strength of this gradation of AC mixture.

Table 3 shows the intermediate principal stresses and failure stresses at the peak points of different gradations, and the peak intermediate principal stress influence factor, b_m, when the minimum principal stress $\sigma_3 = 2$ MPa.

Table 3. Principal stress combination of AC-13 mixtures with different gradation.

Gradation Types	Intermediate Principal Stress Corresponding to Peak Point/MPa	Failure Stress Corresponding to Peak Point/MPa	b_m
AC-13F*	40	55.64	0.708
AC-13M	40	55.93	0.705
AC-13C	38	57.96	0.643

From this table, AC-13C mixture's failure stress is the largest and its intermediate principal stress factor at the peak point is the smallest, suggesting that the curve for the intermediate principal stress σ_2 of AC-13C mixture from σ_2 to arrive at the peak point is the steepest, i.e., the curve has the largest slope. Hence, a coarser gradation will mean a greater effect of intermediate principal stress on its failure strength.

4. Effect of Intermediate Principal Stress on the Compressive Strength of Cement-Stabilized Macadam

Triaxial tests were carried out with a self-developed true triaxial test machine for cement-stabilized macadam specimens with cement content of 3.5%, 4.5% and 5.5%. In the test, the minimum principal stress was set at $\sigma_3 = 2$ MPa, 5 MPa and 8 MPa, and σ_2 was set between the minimum principal stress and the maximum principal stress.

Based on the test results, a figure was developed to show the failure stresses under different cement contents as shown in Figure 6.
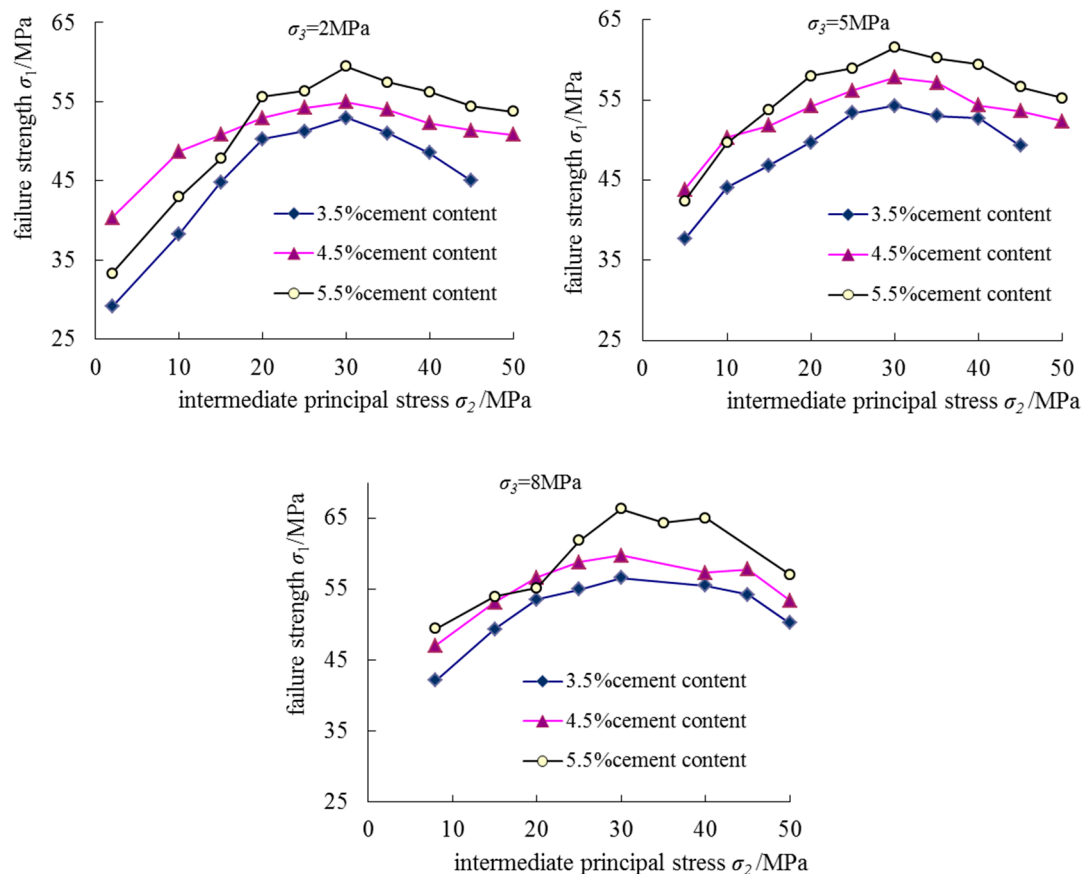

Figure 6. The principal stress effect on the cement stabilized macadam strength of different cement dosage.

Figure 6 demonstrates a distinct effect of the intermediate principal stress on the compressive strength of cement-stabilized macadam: as the intermediate principal stress increases, so does the strength of cement-stabilized macadam; after the intermediate principal stress reaches a given level, the strength of the material starts to decrease, suggesting an interval feature of the effect of intermediate principal stress on the strength of cement-stabilized macadam.

Based on the test results above, the impact of the intermediate principal factor, b, on the failure strength of cement-stabilized macadam was analyzed. The definition of *b* is the same as before.

The same as the previous section, the intermediate principal stress influence factor at the peak point, b_m, was introduced to explain the degree of effect of intermediate principal stress on the failure strength of different content cement-stabilized macadam. Table 4 gives the failure stresses and intermediate principal stresses at peak points and the factor b_m.

From Figure 6 and Table 4:

a. For the same cement-stabilized macadam, the larger the minimum principal stress, the larger the failure strength;

b. For the same gradation of cement-stabilized macadam, as a general rule, as the cement content increases, the failure stress at the peak point increases while the intermediate principal stress influence factor at the peak point, bm, reduces. This suggests that larger cement content means a greater effect of intermediate principal stress on the strength of cement-stabilized macadam.

Table 4. Intermediate principal stress on the compressive strength of cement stabilized macadam.

Cement Content	Minimum Principal Stress/MPa	Peak Intermediate Principle Stress Influence Factor b_m	Failure Stress Corresponding to the Peak Point/MPa
	2	0.49	58.75
5.5%	5	0.44	61.38
	8	0.38	65.26
	2	0.53	54.97
4.5%	5	0.47	57.89
	8	0.43	60.58
	2	0.55	52.79
3.5%	5	0.51	54.32
	8	0.45	56.95

5. Discussion

All the curves in Figures 3–5 show that the compressive strength of AC-13 and cement-stabilized macadam in a complex stress state is very different to that from the uniaxial compression test. However, uniaxial strength theory is still the mainstream methods to design pavements structure and materials. For example, the stress at one direction of a point in pavements is always calculated to compare with its material's uniaxial strength, which is used as the failure criteria for pavement design. In fact, any point inside pavements is in a three-dimensional stress state. The stress state is different between the calculating point and uniaxial strength test, which will result in design error. Therefore, more complex strength theory should be introduced to evaluate pavement materials' performance, such as the strength theory considering all of the three-principal stress.

It has been proved that intermediate principal stress has a great influence on the strength of AC-13 and cement-stabilized macadam. In this section, how to use the results will be discussed. Since the strength model had been developed for AC-13 in Reference [15], only the cement-stabilized macadam's strength model will be discussed here.

Many scholars have proposed various strength models for engineering materials. Several strength models considering the effect of intermediate principal stress will be discussed on its applicability for cement stabilized macadam at following, which include a Mohr–Coulomb model, Double-Shear-Corner Model and Double-Shear Model.

The coordinate system (σ_1, σ_2, σ_3) in principal stress space will be converted to a cylindrical coordinate system (ξ, r, θ) which includes hydrostatic stress axis ξ and π plane. A π plane can be determined by ξ, θ and r represents the stress angle and radius vector on a π plane respectively. There is a corresponding limit curve on a π plane, which represents the strength boundary on that π plane. When the value of r calculating with test data (σ_1, σ_2, σ_3) is greater than the value $r(\theta)$ on failure (ξ, θ), it means the structure or material will be in a state of failure.

For comparison purposes, $r(\theta)$ will be nondimensionalized as follows:

$$g(\theta) = r(\theta)/r(60°), \tag{1}$$

where $r(\theta)$ is the radius vector on a π plane when stress angle is θ, and

$$\text{tg}\theta = \sqrt{3}(\sigma_1 - \sigma_2)/(\sigma_1 + \sigma_2 - 2\sigma_3). \tag{2}$$

Based on the strength data of different cement content cement-stabilized macadam, its θ, $r(\theta)$ and $r(60°)$ can be directly calculated. Then, the limit curve $g(\theta)$ based on measured data can be obtained. This limit curve $g(\theta)$ will be compared with strength models. The $g(\theta)$ of the Mohr–Coulomb model, Double-Shear-Corner Model and the Double-Shear Model will be calculated with test data θ according to relevant equations in Reference [25]. The calculating results are shown in Tables 5–7.

Table 5. The $g(\theta)$ on π plane which hydrostatic stress is 34 MPa for 5.5% cement content cement-stabilized macadam.

$g(\theta)$	9.7°	16.9°	19°	27.1°	38.1°	60°
Calculating directly with test data	0.868	0.865	0.830	0.860	0.915	1
Calculation value with Mohr–Coulomb model	0.787	0.775	0.773	0.778	0.810	1
Calculation value with Double Shear Corner Model	0.834	0.850	0.856	0.885	0.933	1
Calculation value with Double Shear Model	0.838	0.863	0.874	0.928	1.048	1

Table 6. The $g(\theta)$ on π plane whose hydrostatic stress is 32.8 MPa for 4.5% cement content cement-stabilized macadam.

$g(\theta)$	6.8°	16.4°	25°	42.8°	60°
Calculating directly with test data	0.918	0.867	0.894	0.981	1
Calculation value with Mohr–Coulomb model	0.803	0.781	0.780	0.837	1
Calculation value with Double Shear Corner Model	0.838	0.856	0.883	0.958	1
Calculation value with Double Shear Model	0.840	0.870	0.921	1.047	1

Table 7. The $g(\theta)$ on π plane whose hydrostatic stress is 30.9 MPa for 3.5% cement content cement-stabilized macadam.

$g(\theta)$	9.9°	14.9°	21.8°	33.1°	60°
Calculating directly with test data	0.959	0.957	0.940	0.942	1
Calculation value with Mohr–Coulomb model	0.893	0.872	0.854	0.852	1
Calculation value with Double Shear Corner Model	0.965	0.968	0.973	0.984	1
Calculation value with Double Shear Model	0.976	0.995	1.036	1.000	1

From Tables 5–7, it can not be found intuitively which model is more suitable to characterize the strength performance of cement-stabilized macadam. Mathematical analysis methods were applied to compare the group data in Tables 5–7. The Residual Sum of Squares Q between $g(\theta)$ from test data and from three known models was calculated, respectively. Q represents the dispersion degree of the $g(\theta)$ based on test data from the model curve $g(\theta)$. The larger the Q value, the greater the dispersion degree.

It can be observed from Table 8 that the Double-Shear-Corner Model is the most suitable model in the three models to characterize the strength performance of cement-stabilized macadam. Even for a relatively advanced model, the Mohr–Coulomb model, being applied in pavement fields, its application to characterize cement-stabilized macadam's strength performance will also result in a large error.

Table 8. The residual sum of squares between $g(\theta)$ from test data and from three known models.

Cement-Stabilized Macadam　　　Known Models	Mohr–Coulomb Model	Double-Shear-Corner Model	Double-Shear-Model
5.5% cement content	0.036	0.003	0.025
4.5% cement content	0.054	0.007	0.011
3.5% cement content	0.027	0.003	0.014

6. Conclusions

(1) True triaxial compression test on different gradations of AC-13 mixture and cement-stabilized macadam indicates that intermediate principal stress has a role to play in the failure strength of pavement materials, and this effect has an interval. That is, as the intermediate principal stress increases, the compressive strength increases first and then reduces.

(2) Under triaxial compression, the minimum principal stress has influence on the compressive strength of cement-stabilized materials: a larger minimum principal stress will result in a greater compressive strength.

(3) For AC-13 mixture, gradation differences do not make much difference to its triaxial compressive strength except that a coarser gradation means greater impact of intermediate principal stress on its compressive strength.

(4) For cement-stabilized macadam, as the cement content increases, the strength at the peak point increases while the intermediate principal stress influence factor, b_m, reduces, suggesting that intermediate principal stress is more effective on the strength of cement-stabilized macadam with higher cement content.

(5) Compared with the Mohr–Coulomb model and Double-Shear Model, the Double-Shear-Corner Model is more suitable to characterize a cement-stabilized macadam's strength performance.

This paper only addresses triaxial compressive strength, yet tensile-compressive stresses' combination condition also exists in the pavement structures, and strength tests under more complex stress combinations will be one of the targets for subsequent studies.

Author Contributions: H.-x.G. conceived and designed the experiments, H.L. and J.-j.Y. performed the experiments, H.-x.G. and H.-q.W. analyzed the data, and H.-X.G. and M.L. wrote the paper.

Conflicts of Interest: The authors declare no conflict of interest.

References

1. Ma, S.K.; Huang, M.S.; Hu, P.; Yang, C. Soil-water characteristics and shear strength in constant water content triaxial tests on Yunnan red clay. *J. Cent. South Univ.* **2013**, *20*, 1412–1419. [CrossRef]

2. Li, H.Z.; Liao, H.J. Anisotropy of Strength of Rock Mass under Complicated Stress State. *Chin. J. Rock Mech. Eng.* **2010**, *29*, 1397–1403.

3. Wang, H.L.; Song, Y.P. Behavior of Mass Concrete under Biaxial Compression-tension and Triaxial Compression-tension. *Mater. Struct.* **2009**, *42*, 241–249. [CrossRef]

4. Rukhaiyar, S.; Sajwan, G.; Samadhiya, N.K. Strength behavior of plain cement concrete subjected to true triaxial compression. *Can. J. Civ. Eng.* **2018**, *45*, 179–196. [CrossRef]

5. Shang, H.S.; Ji, G.J. Mechanical behavior of different types of concrete under multiaxial compression. Mag. Concr. Res. **2014**, *66*, 870–876. [CrossRef]

6. Rukhaiyar, S.; Samadhiya, N.K. Strength behaviour of sandstone subjected to polyaxial state of stress. *Int. J. Min. Sci. Technol.* **2017**, *27*, 889–897. [CrossRef]

7. Yin, J.H.; Cheng, C.M.; Kumruzzaman, M.; Zhou, W.H. New Mixed Boundary, True Triaxial Loading Device for Testing Three-dimensional stress-strain- strength Behavior of Geomaterials. *Can. Geotechnol. J.* **2010**, *47*, 1–15. [CrossRef]

8. Shi, W.C.; Zhu, J.G.; Liu, H.L. Influence of Intermediate Principal Stress on Deformation and Strength of Gravel. *Chin. J. Geotech. Eng.;* **2008**, *30*, 1449–1453.

9. Shi, W.C.; Zhu, J.G.; Chiu, C.F.; Liu, H.L. Strength and deformation behavior of coarse-grained soil by true triaxial tests. *J. Cent. South Univ. Technol.* **2010**, *5*, 1095–1102. [CrossRef]

10. Eghbali, A.H.; Fakharian, K. Effect of principal stress rotation in cement-treated sands using triaxial and simple shear tests. *Int. J. Civ. Eng.* **2014**, *12*, 1–14.

11. Jia, Z.J.; Long, P.J.; Ying, L.C.K.; Jin, L.Z. Experimental study on mechanical behavior of high performance concrete under multi-axial compressive stress. *Sci. China Technol. Sci.* **2014**, *57*, 2514–2522.

12. He, Z.J.; Cao, W.L.; Zhang, J.X.; Wang, L. Multiaxial mechanical properties of plain recycled aggregate concrete. *Mag. Concr. Res.* **2015**, *67*, 401–413. [CrossRef]

13. Phusing, D.; Suzuki, K.; Zaman, M. Mechanical Behavior of Granular Materials under Continuously Varying b Values Using DEM. *Int. J. Geomech.* **2015**, *16*, 1–12. [CrossRef]

14. Xiao, Y.; Liu, H.; Sun, Y.; Liu, H.; Chen, Y. Stress–dilatancy behaviors of coarse granular soils in three-dimensional stress space. *Eng. Geol.* **2015**, *195*, 104–110. [CrossRef]

15. Guan, H.X.; Li, L.Y.; Yang, H.Y. The Intermediate Principal Stress Effect on Asphalt Mixture. *China J. Highway Transp.* **2014**, *27*, 11–16.

16. Suo, L.; Tong, H.; Wang, B. Influence of Intermediate Principal Stress on Asphalt Mixture Strength in Positive Temperature. *J. Chang'an Univ.* **2011**, *31*, 12–16.

17. Wang, L.; Hoyos, L.R.; Wang, J.; Voyiadjis, G.; Abadie, C. Anisotropic Properties of Asphalt Concrete: Characterization and Implications for Pavement Design and Analysis. *J. Mater. Civ. Eng.* **2005**, *17*, 535–543. [CrossRef]

18. Song, X.J.; Xu, H.B.; Wang, Y.L.; Wang, W.; Zhou, A.Z. Study of the Characteristics of Cement-soil Anisotropic Deformation. *Rock Soil Mech.* **2012**, *33*, 1619–1624.

19. Huang, T.; Li, Y.P.; Zheng, J.L. Intermediate principal stress effect and failure criterion of asphalt mixture under triaxial compression state. *J. Cent. South Univ.* **2016**, *47*, 3225–3230.

20. Huang, T.; Chang, Z.D.; Yang, Y. Failure criterion of asphalt mixture in triaxial tension and compression state. *J. Cent. South Univ.* **2017**, *48*, 1908–1914.

21. Yang, Q.; Chen, L.; Wang, P.; Dai, J. New Asphalt Pavement Failure Criterion Based on Unified Strength Theory. *J. Wuhan Univ. Technol.* **2015**, *30*, 528–532. [CrossRef]

22. *Technical Specifications for Construction of Highway Asphalt Pavements*; China Communications Press: Beijing, China, 2004; JTG F40-2004; p. 26.

23. *Test Methds of Materials Stabilized with Inorganic Binders of Highway Engineering*; China Communications Press: Beijing, China, 2009; JTG E51-2009; p. 93.

24. Li, Z.; Zhang, H.; Hou, Y.; Tian, X. Triaxial Test Study on Mechanical Characteristics of Asphalt Concrete in the Core Wall of Earth-rock Fill Dam. *Chin. J. Rock Mech. Eng.* **2006**, *25*, 997–1002.

25. Yu, M.H. *Strength Theories New System: Theories Development and Applying*; Xi'an Jiaotong University Press: Xi'an, China, 2011.